scientific reports

Check for updates

OPEN

Expression of Wnt signaling proteins LEF1, β-catenin, GSK3β, DVL1, and N-myc varies across retinoblastoma subtypes and pRb phosphorylation status

Leon Marković[1,2], Anja Bukovac[3,4], Ana Maria Varošanec[1,2], Antonia Jakovčević[5], Davor Tomas[5], Zdenko Sonicki[6], Borna Puljko[4,7], Fran Dumančić[3,4], Reno Hrašćan[8] & Nives Pećina-Šlaus[3,4]✉

Retinoblastoma, a rare childhood eye cancer, has hereditary and non-hereditary forms. While TNM classification helps in prognosis, understanding molecular mechanisms is vital for the clinical behavior of retinoblastoma prediction. Our study aimed to analyze the expression levels of key Wnt pathway proteins, GSK3β, LEF1, β-catenin, and DVL1, and associate them to non-phosphorylated active form (pRb) and the phosphorylated inactive form (ppRb) and N-myc expression, in retinoblastoma cells and healthy retinal cells, in order to elucidate their roles in retinoblastoma and identify potential targets that could help to improve diagnostic and therapy. Specimens from 22 retinoblastoma cases (unilateral, bilateral, and trilateral) were analyzed. Immunohistochemistry assessed proteins' expressions, followed by semi-quantitative analysis using the Immunoreactivity Score (IRS). Bayesian statistical methods were employed for data analysis. The study revealed various expression patterns of Wnt signaling proteins across different retinoblastoma types. The high expression levels were observed for LEF1 and DVL1. Inactive GSK3β and nuclear localization of β-catenin indicated Wnt signaling activation. The levels of inactive ppRb were significantly higher in retinoblastoma compared to healthy retina, as well as the levels of inactive GSK3β. Positive correlations between DVL1 and N-myc, GSK3β Y216 and GSK3β S9 and non-P β-catenin and LEF1 were established. Retinoblastomas without germline mutations (*RB1*$^{+/+}$) exhibited high pRb, N-myc, and LEF1 levels, while those in genetically predisposed children (*RB1*$^{+}$*/-)* showed lower expression of these proteins. Trilateral retinoblastomas demonstrated especially high N-myc and LEF1, but low pRb and ppRb levels. The findings highlight the meaningful role of the Wnt signaling pathway in retinoblastoma pathogenesis, providing insights into potential therapeutic targets. Understanding molecular features may pave the way for personalized treatments and improve outcomes for retinoblastoma patients.

Keywords Retinoblastoma, Wnt signaling pathway, *RB1*, pRb, ppRb, N-myc, LEF1, β-catenin, DVL1, GSK3β

Abbreviations

AJCC	American Joint Committee on Cancer
BF	Bayesian factor

[1]Department of Ophthalmology, Reference Center of the Ministry of Health of the Republic of Croatia for Pediatric Ophthalmology and Strabismus, University Hospital "Sveti Duh", Zagreb, Croatia. [2]Faculty of Dental Medicine and Health Osijek, Josip Juraj Strossmayer University of Osijek, Osijek, Croatia. [3]Department of Biology, School of Medicine, University of Zagreb, Salata 3, 10000 Zagreb, Croatia. [4]Croatian Institute for Brain Research School of Medicine, University of Zagreb, Zagreb, Croatia. [5]Department of Pathology and Cytology Ljudevit Jurak, University Hospital Center Sestre Milosrdnice, Zagreb, Croatia. [6]Department of Medical Statistics, Epidemiology and Medical Informatics, Andrija Štampar School of Public Health, University of Zagreb, School of Medicine, Zagreb, Croatia. [7]Department of Chemistry and Biochemistry, School of Medicine, University of Zagreb, Zagreb, Croatia. [8]Department of Biochemical Engineering, Faculty of Food Technology and Biotechnology, University of Zagreb, 10000 Zagreb, Croatia. ✉email: nina@mef.hr

CDK	Cyclin-dependent kinase
Dvl	Disheveled protein family
DVL1	Disheveled 1
E2F	E2 Transcription factor
FFPE	Formalin-fixed paraffin-embedded
GSK3β	Glycogen synthase kinase 3 beta
IRS	Immunoreactivity score
LEF1	Lymphoid enhancer-binding factor 1
LRP	LDL receptor-related protein
LEF1-AS1	LEF1 antisense RNA 1
N-myc	N-Myc proto-oncogene protein
pRb	Retinoblastoma protein (non-phosphorylated form)
ppRb	Retinoblastoma protein (phosphorylated inactive form)
RB1	Retinoblastoma 1 gene
Ser9	Serine 9
Ser807	Serine 807
Ser811	Serine 811
T2b	Tumor size/extent category in TNM staging
TNM	Tumor, node, metastasis classification
Y216	Tyrosine 216

Retinoblastoma is a relatively rare primary intraocular malignancy in children, occurring in 1:15,000–1:20,000 live births and approximately 9,000 new cases per year, mostly in Asia and Africa. It is the most common primary intraocular malignancy in childhood, accounting for 3% of all childhood tumors[1]. There are two forms of retinoblastoma: hereditary (familial) and non-hereditary (sporadic). Hereditary forms occur in about 40% of cases, while non-hereditary forms occur in about 60%[2]. The diagnosis of retinoblastoma is typically made within the first year of life for patients with bilateral disease and within 3 years for those with unilateral disease[3].

Recently, the evaluation of the eighth version of the TNM classification for retinoblastomas, developed by the American Joint Committee on Cancer, has led to significant advancements in understanding and predicting the mortality associated with retinoblastoma. Significant new research has resulted in a new TNM classification system that is more effective in assessing the prognosis of retinoblastoma based on factors such as tumor size, lymph node involvement, metastasis presence, and inheritance pattern[4].

Retinoblastomas arise due to the loss or mutation of both alleles of the *RB1* tumor suppressor gene, which encodes pRb phosphoprotein[5]. pRb plays a crucial role in regulating cell cycle progression, and its functional inactivation is a critical step in the development of retinoblastoma. It is important to note that pRb can be inactivated by various mechanisms including mutations and phosphorylation. Currently, it is well-established that retinoblastoma protein (pRb) demonstrates distinct activity states when phosphorylated at Ser807 and Ser811, or at both sites. Phosphorylation of the pRb promotes G1/S cell cycle progression. This diversity in phosphorylation patterns of active pRb in human retinoblastoma results in varied effects on its cellular function[6]. Consequently, dysregulation of the pRb/E2F pathway is implicated in the transformation and progression of healthy retinal cells into retinoblastoma cells[7].

Although other signaling pathways may also be involved, the Wnt pathway has been indicated as a novel player in the etiology of retinoblastoma. A small number of studies have investigated the involvement of Wnt signaling in retinoblastoma development and progression, and the roles of individual genes and proteins remain incompletely characterized, especially their effect on retinoblastoma clinical behavior[8]. Therefore, further research is needed to elucidate the exact role of this pathway in retinoblastoma.

Specifically, we have selected several pivotal regulators of the Wnt pathway, namely GSK3β, LEF1, β-catenin, and DVL1 based on two things. Firstly, several literature reports that indicated findings on Wnt signaling involvement[8–13] and secondly from our previous work on neural tumor tissue, primarily astrocytoma, where we observed changes in the expression patterns of those specific molecules[14–16].

Structural variations and mutations in Wnt signaling genes have been linked to retinoblastoma[17]. Wnt gene expression in the retina has been shown to alter the Wnt signaling in retinoblastoma, and Wnt signaling is known to regulate the proliferation and differentiation of retinal stem/progenitor cells[18]. Recent studies in human and mouse retinoblastoma cell lines have explored Wnt signaling's role in tumor growth[8,10,11]. For instance, Tell et al. found that Wnt signaling protects healthy retinal cells by preventing uncontrolled proliferation[8]. Xiao et al. demonstrated that inhibiting the Notch pathway halted the proliferation of retinoblastoma cells by suppressing the Wnt pathway. Li et al. investigated Wnt inhibition, showing that drugs like niclosamide and miR-485 could reduce tumor growth[11].

Additionally, long non-coding RNAs (lncRNAs) have been shown to modulate Wnt signaling in retinoblastoma[18]. Studies identified oncogenic lncRNAs like LEF1-AS1[12], which is associated with poor prognosis, while tumor-suppressive lncRNAs, like MEG3, inhibit Wnt signaling by promoting β-catenin degradation[19]. Other studies highlighted the Wnt pathway regulator DKK3, whose overexpression suppresses tumor growth by inducing cell cycle arrest and apoptosis in retinoblastoma cells[20].

The *MYCN* gene, known for its role in neuroblastoma, has also been implicated in a rare subtype of retinoblastoma with intact *RB1* genes. *MYCN* amplification is linked to aggressive tumor behavior and poor prognosis[21], prompting its inclusion in ongoing research.

The aforementioned research underscores the potential role of the Wnt signaling pathway in retinoblastoma development, though the specific functions of key components remain unclear. Our aim is to investigate the expression levels of pRb (wild type and phosphorylated), N-Myc, LEF1, DVL1, β-catenin, and GSK3β,

comparing these between retinoblastoma and healthy retinal cells. By using specific antibodies to detect active and inactive protein forms, we will correlate β-catenin activity, as well as pRb and GSK3β phosphorylation, with other proteins and clinical parameters. This analysis aims to enhance our understanding of retinoblastoma's molecular profile and uncover potential therapeutic targets.

Importantly, this study may have clinical implications. New biomarkers could improve diagnostics and provide insight into retinoblastoma's clinical behavior, particularly in understanding why certain tumors exhibit chemoresistance. Identifying novel therapeutic targets within the Wnt pathway offers a promising avenue for future treatment strategies in retinoblastoma patients.

Materials and methods

Retinoblastoma specimens

Specimens from 22 cases of human retinoblastoma and 20 healthy eyes were gathered from pathology departments spanning hospitals across the Republic of Croatia. Specifically, tumors were sourced from the Clinical Department of Pathology and Cytology at the University Hospital Center Zagreb, Croatia, the Department of Pathology and Cytology "Ljudevit Jurak," situated within the University Hospital Center "Sestre milosrdnice," Zagreb, Croatia, and from the Department of Pathology and Cytology, University Hospital "Sveti Duh," Zagreb, Croatia, subsequent to enucleation procedures. These tumors were localized within the tissue of enucleated eyes from patients diagnosed with retinoblastoma. Following collection, all tumors underwent thorough histopathological scrutiny by specialized pathologists and were classified in accordance with the 8th edition of the TNM classification established by the American Joint Committee on Cancer (AJCC)[4].

Retrospectively, data on age, gender, available genetic testing, and the date of enucleation were collected.

The Ethics Committees of the School of Medicine, University of Zagreb (Case number: 380–59-10,106–20-111/126; Class: 641–01/20–02/01), University Hospital Center Zagreb (Case number: 02/21 AG; Class: 8.1–20/108–2), University Hospital Center „Sestre Milosrdnice " (Case number: 251–29-11–20-01–9; Class: 003–06/20–03/015), and Univerity Hospital „Sveti Duh" (Case number: 012–5477) have approved the research. The study adhered to the principles outlined in the Declaration of Helsinki.

Immunohistochemistry

Immunohistochemistry was conducted to assess the presence and expression levels of pRb, ppRb, N-myc, LEF1, DVL1, β-catenin, and GSK3β. The samples consisted of 4-µm FFPE sections affixed to capillary gap microscope slides from DakoCytomation, Glostrup, Denmark. The immunohistochemistry protocol was outlined previously[9]. Details regarding the antibodies and their dilutions are provided in Supplementary Table S1. The antibodies have passed rigorous application-specific testing standards.

The sections were subjected to immunostaining using peroxidase/DAB + (3,3-diaminobenzidine) from Dako REAL™ EnVision™, Glostrup, Denmark. Evaluation of expression levels in healthy eyes retinal tissue was conducted using enucleated human eyes, which underwent the identical immunohistochemistry process as the sections from retinoblastoma tissues. Positive controls included human liver cancer, colon cancer tissue, prostate cancer tissue, thyroid tissue, and normal bronchial epithelia. Negative controls underwent the same staining procedure but without incubating samples with primary antibodies. Antibodies employed were evaluated on positive controls by western blot.

Antibody labeling was analyzed by two independent observers who were blinded to the experimental conditions, using an Olympus BX53 microscope. ImageJ software from the National Institutes of Health, Bethesda, Maryland, USA, was employed to determine cell numbers and protein expression intensities. To measure the level of agreement between their assessments, we conducted a kappa statistic analysis. The computed kappa value was 0.66, which indicates substantial agreement. This result demonstrates a strong level of consistency in the pathologists' scoring.

A minimum of 300 cells were counted in the tumor hot spot area at a magnification of 200× for semi-quantitative analysis. Using ImageJ (National Institutes of Health, USA), the assessment of immunopositivity was based on the IRS score (Immunoreactivity Score). The IRS score is a metric that strongly aligns with computational photo analysis. It is computed by multiplying the percentage of cells exhibiting a positive signal in the sample (PP score) by the staining intensity (SI score). The PP score is classified as follows: no immunopositivity in tumor cells (score 0), 1–25% positive cells (score 1), > 25–50% (score 2), > 50–90% (score 3), and > 90% (score 4). Meanwhile, the SI score is evaluated across three categories: no staining or weak (score 1), moderate staining (score 2), and strong staining (score 3). In our study, the IRS ranged from 0 to 12.

Statistical analysis

Statistical analyses were conducted using Bayesian methods. The Bayesian approach was selected because it is particularly effective when handling small sample sizes, its ability to incorporate prior knowledge, its flexibility in modeling complex data, and its more comprehensive treatment of uncertainty—all of which are especially relevant in the research of rare conditions like retinoblastoma. Bayesian independent sample t-tests was used to compare different expression patterns between healthy retinal tissue, retinal tissue surrounding retinoblastoma and retinoblastoma tissue. Bayesian correlation was used to correlate demographic, genetic and patohistological characteristics with protein expression levels. All analyses were two-tailed and were carried out using JASP (Jeffreys's Amazing Statistics Program), version 0.18.3.

Results

Retinoblastoma cases demographic, patohistological characteristics and mutational status

The study analyzed 22 retinoblastoma tumors, categorized at enucleation into unilateral (14 eyes, average size 1.6 cm, mostly cT1a and cT2b, mostly H0), bilateral (6 eyes, average size 2.0 cm, diverse TNM classifications, all H1), and trilateral types (2 eyes, average size 2.7 cm, cT2b and cT3b, both H1). The male-to-female ratio was higher in unilateral and bilateral types. The TNM classification indicated that unilateral retinoblastomas tended to have lower grades, with 43% of these cases exhibiting cT1a. In contrast, bilateral and trilateral retinoblastoma subtypes did not show any cT1a cases. Specifically, trilateral retinoblastomas were exclusively classified as cT2b and cT3a, Table 1.

Histopathological features are indicated in Table S2 together with germline mutations and those found in tumor tissue.

A statistical analysis was conducted to assess correlations between the expression levels of our markers and both the tumor stages defined by the 8th edition of the TNM classification, as well as key histopathological risk factors, including differentiation (poor, moderate, and well), anaplasia (mild, moderate, and severe), and invasion (choroid and optic nerve). However, none of these correlations yielded significant associations with the marker expression levels.

Supplementary Table S2 summarizes the demographic data, histopathological characteristics, and mutational profiles of the analyzed retinoblastoma samples.

Immunohistochemical staining patterns

Examining cellular protein expression in retinoblastoma and the surrounding retinal tissue, as well as healthy eyes retinal tissue, pRb displayed the highest IRS scores in unilateral retinoblastoma (IRS = 8) and the adjacent retina (IRS = 7). Conversely, the lowest pRb levels were observed in trilateral retinoblastoma tissue (IRS = 4). Additionally, ppRb (inactive) expression levels were generally lower across all retinoblastoma subtypes compared to pRb levels. Specifically, higher IRS scores were noted in unilateral and trilateral retinoblastoma (IRS = 4), while similar IRS scores (IRS = 2) were observed in the retina surrounding retinoblastoma tissue across all subtypes. Notably, no expression of ppRb (inactive) was identified in the retina of healthy eyes (IRS = 0).

When comparing the expression levels of the inactive and active forms of GSK3β in retinoblastoma tissue and the surrounding retina, notable differences emerged. Across all retinoblastoma subtypes, higher IRS scores were consistently observed for the inactive form (GSK3β S8) compared to the active form (GSK3β Y216), where IRS scores were lower both within the retinoblastoma tissue and its adjacent tissue. In stark contrast, the retina of healthy eyes exhibited higher cellular expression levels of the active form (GSK3β Y216) (IRS = 8) in comparison to the inactive form (GSK3β S8) (IRS = 2).

Retinoblastoma tissue and the surrounding retina exhibited elevated DVL1 IRS scores, with the highest scores recorded in trilateral retinoblastoma (IRS = 12). Conversely, the retina of healthy eyes displayed minimal DVL1 cellular expression, nearly absent (IRS = 1).

Upon analyzing the expression of non-phospho β-catenin, a distinct localization pattern emerged, within retinoblastoma tissue, the expression was primarily localized in the nucleus, while in the surrounding retina and healthy eyes retina, it predominantly resided in the cytoplasm. This discrepancy suggests varied roles of this protein within the tumor and retinal tissue, Fig. 1. When in nucleus it is indicative of Wnt signaling activation, while when in cytoplasm it participates in adherens junctions formation. Thus, the expression levels in retinoblastoma cells were comparable to those in the retinoblastoma surrounding retinal tissue and healthy eyes' retina, with the highest IRS scores observed in the healthy eyes retina (IRS = 9).

Cellular expression levels of LEF1 were notably highest in trilateral retinoblastoma (IRS = 6), with no discernible expression in the surrounding retinoblastoma tissue and the retina of healthy eyes (IRS = 0).

Similar expression patterns were evident upon analyzing N-myc cellular expression, with the highest IRS observed in trilateral retinoblastoma (IRS = 8), while no expression was detected in the surrounding retina of unilateral retinoblastoma and the retina of healthy eyes (IRS = 0). Unilateral and bilateral cases showed IRS of 3 and 4, respecively, which is higher than the levels found in adjacent retina (Table 2).

Moreover, distinct expression intensities of several proteins were observed in the transitional zone from the retina to retinoblastoma tissue. As depicted in Fig. 2, an elevation in the expression of DVL1, LEF1, and N-myc was noted in retinoblastoma cells compared to retinal cells. Furthermore, retinal cells closer to the retinoblastoma tissue, particularly in the outer nuclear layer (ONL) and internal nuclear layer (INL), exhibited heightened nuclear levels of LEF1 and N-myc proteins, alongside increased cytoplasmic levels of DVL1. Additionally, higher levels of DVL1, LEF1, and N-myc were observed in the INL compared to the ONL.

				TNM classification					
	Number of eyes; (OD/OS)	Male/female	Average tumor size (cm)	cT1a	cT1b	cT2a	cT2b	cT3b	H0/H1
Unilateral retinoblastoma	14;6/8	8/6	1.6 ± 1.1	6	n/a	3	4	1	11/3
Bilateral retinoblastoma	6;4/2	4/2	2.0 ± 0.6	n/a	2	2	1	1	0/6
Trilateral retinoblastoma	2;1/1	2/0	2.7 ± 0.1	n/a	n/a	n/a	1	1	0/2

Table 1. Demographic and patohistological tumor characteristics of retinoblastoma cohort. OD-right eye; OS-left eye; n/a-not applicable.

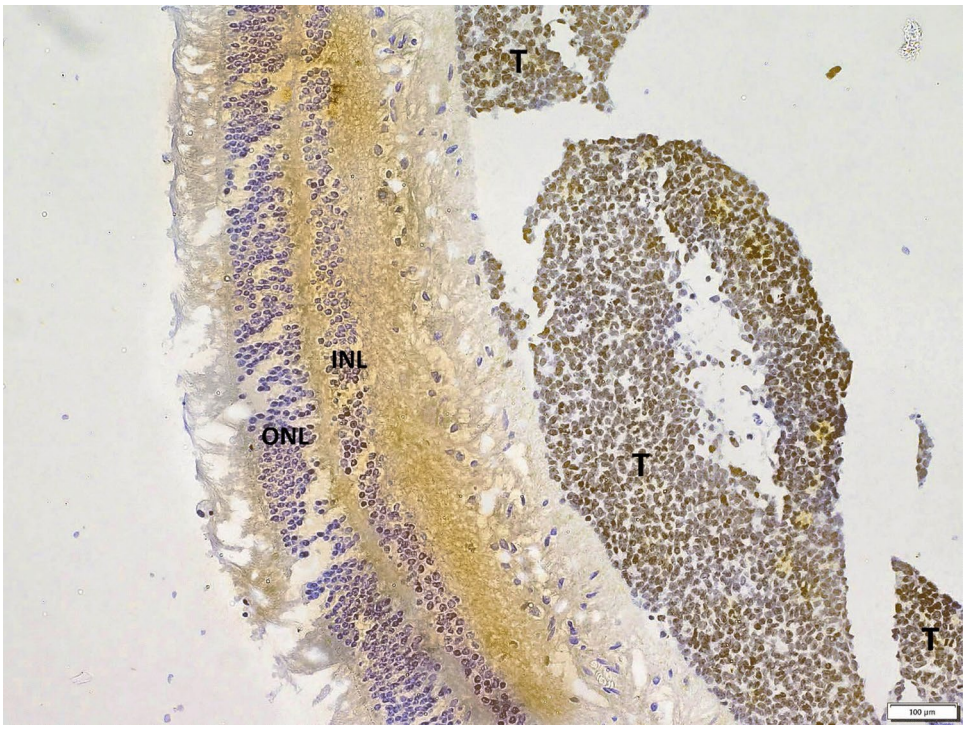

Fig. 1. Different expression patterns of non-phospho (active) β-catenin in retinoblastoma tissue and surrounding retina. Scale bars correspond to 100 µm. Abbreviations: internal nuclear layer (INL), outer nuclear layer (ONL), tumor tissue (T).

	Tumor (IRS score; rounded average)								Retina (IRS score; rounded average)							
	pRb	ppRb	DVL1	GSK3β Y216	GSK3β S9	nonP β-catenin	LEF1	N-myc	pRb	ppRb	DVL1	GSK3β Y216	GSK3β S9	nonP β-catenin	LEF1	N-myc
Unilateral retinoblastoma	8	4	7	6	10	2	4	3	7	2	7	7	10	4	0	0
Bilateral retinoblastoma	6	4	6	5	11	2	4	4	5	2	8	6	10	4	0	1
Trilateral retinoblastoma	4	2	12	6	12	6	6	8	5	2	8	3	12	9	0	1
Healthy eyes									6	0	1	8	2	9	0	0

Table 2. Characteristics of different retinoblastoma tumor types, retina surrounding retinoblastoma tumors and normal healthy retina immunostained with antibodies against pRb, ppRb, DVL1, GSK3β S9, GSK3β Y216, non-phospho β-catenin, LEF1 and N-myc.

Table 2 provides a comprehensive overview of the detailed IRS scores for various retinoblastoma subtypes, as well as the retina surrounding retinoblastoma and the retina of healthy eyes.

Comparative analysis of protein expression in different types of retinoblastoma and healthy eyes

Comparing the cellular expression levels of various proteins in retinoblastoma tissue, the surrounding retina, and the retina of healthy eyes, notable distinctions were observed. The highest IRS scores for pRb were associated to unilateral retinoblastoma (IRS = 8) and the adjacent retina (IRS = 7), and the lowest pRb score (IRS = 4) was observed in trilateral retinoblastoma. While the expression of pRb suggests no significant difference in retinoblastoma compared to the healthy eye retina, indicated by lower Bayesian factors, the levels of ppRb (inactive) expression reveal a notable disparity between retinoblastoma tissue and the healthy eyes' retina where levels of inacitve ppRb were significantly higher in retinoblastoma. Higher Bayesian factors are detected in both the retinoblastoma tissue and the retinoblastoma surrounding retina, especially in the bilateral subtype.

Moreover, the expression of GSK3β Y216, representing the active form, is associated with lower Bayesian factors, suggesting no significant difference between retinoblastoma and the healthy eyes retina. On the other hand, the prevalence of GSK3β S9 (inactive form) expression across all retinoblastoma subtypes is highlighted by notably high Bayesian factors, indicating a significant difference compared to the healthy eyes' retina. Notably, when comparing the retina surrounding retinoblastoma and the retina of healthy eyes, GSK3β S9 expression

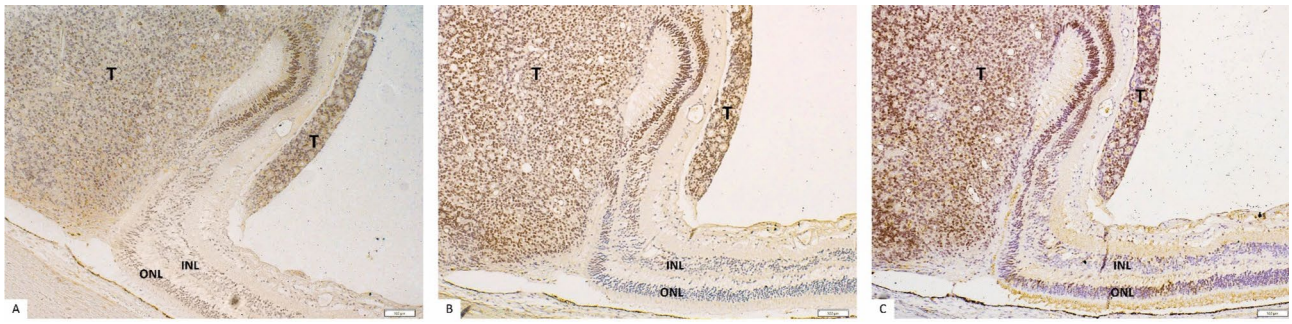

Fig. 2. Transitional zone from the retina to retinoblastoma in trilateral retinoblastoma, immunostained with antibodies against DVL1 (**A**), LEF1 (**B**) and N-myc (**C**). The images show tumor cells expressing higher levels of DVL1, LEF1 and N-myc compared to retinal cells. The majority of cells in the region of the expanding tumors show moderate-to-strong reactivity for DVL1, LEF1 and N-myc compared to the adjacent retinal tissue. Only the retinal cell adjacent to retinoblastoma exhibits higher expression of DVL1, LEF1 and N-myc. Scale bars correspond to 100 µm. Abbreviations: internal nuclear layer (INL), outer nuclear layer (ONL), tumor tissue (T).

reveals a significant difference between different retinoblastoma types and healthy eyes retina. However, differences among various retinoblastoma subtypes did not exhibit a significant disparity in cellular expression levels within the tumor and the surrounding retinal tissue.

Additionally, DVL1 demonstrated notable disparities in expression levels between tumor tissue and the retina of healthy eyes, with remarkably high Bayesian factors across all retinoblastoma types, indicating a significant difference compared to the healthy eye retina. Furthermore, the expression of DVL1 within retinoblastoma cells reveals distinct variations between unilateral and bilateral retinoblastoma when compared to trilateral retinoblastoma, as evidenced by higher Bayesian factors.

Similarly, nonP (active) β-catenin expression in retinoblastoma and the retina surrounding retinoblastoma shows substantial Bayesian factors for all retinoblastoma types, indicating a significant difference compared to the healthy retina. However, when comparing the tumor surrounding retina to the retina from healthy eyes, lower Bayesian factors were observed.

Regarding LEF1 expression, higher Bayesian factors across all retinoblastoma types in the tumor indicate a significant difference compared to the healthy eye retina. However, lower Bayesian factors are observed when comparing the retina surrounding retinoblastoma and healty eye retina, suggesting no significant difference.

Furthermore, comparing N-myc expression in retinoblastoma tissue and healthy eyes' retina, indicated a significant difference demonstrated by higher Bayesian factors for all retinoblastoma types. Lastly, N-myc expression in the tumor illustrates a significant difference between unilateral and trilateral retinoblastoma, as indicated by very high Bayesian factors. N-myc expression was much lower in unilateral retinoblastoma (IRS = 3) compared to trilateral retinoblastoma (IRS = 8).

A comprehensive comparison is presented in Fig. 3, Supplementary Table S3, and Supplementary Table S4.

Comparative analysis of protein expression levels in retinoblastoma tissue

The Bayesian correlation of expression of proteins in retinoblastoma reveals significant relationships between various factors. DVL1 and N-myc show a strong positive correlation (Pearson's r: 0.465; BF10: 2.471), indicating a significant association between these two proteins in retinoblastoma. Similarly, GSK3β Y216 and GSK3β S9 also show a strong positive correlation (Pearson's r: 0.407; BF10: 1.390), suggesting these two phosphorylated forms may interact in the disease process. Furthermore, a significant correlation (Pearson's r: 0.770; BF10: 982.387) has been established between non-P β-catenin and LEF1.

A more detailed comparison is included in Supplementary Table S5.

Expression of pRB, ppRB, LEF1 and N-myc in unilateral, bilateral and trilateral retinoblastoma based on different *RB1* mutation status

Retrospective data based on blood sample genetic testing for *RB1* germline mutation was collected. Based on these findings, the highest percentage (78%) of unilateral retinoblastoma had no detectable germline mutations ($RB1^{+/+}$) when DNA from tumor retinal cells and from blood were compared. Types of germline and somatic mutation found in our patients are shown in Supplementaly Table S2. In cases of bilateral retinoblastoma, the majority exhibited a single mutated allele in the blood (germline mutation) ($RB1^{+/-}$). In trilateral retinoblastoma, both specimens exhibited a germline mutation ($RB1^{+/-}$), however, one specimen also presented a somatic mutation. Our analysis showed that retinoblastoma patients without germline mutation ($RB1^{+/+}$) expressed high levels of pRb, N-myc and LEF1. In all types of retinoblastoma with a single or both *RB1* mutations, the expression of pRb and ppRb is lower, accompanied with lower expression of both N-myc and LEF1. Additionally, in trilateral retinoblastoma, a low expression of pRb and ppRb was observed, with very high expression values of N-myc and LEF1, Table 3.

Characterizing the expression levels of pRB, ppRB, N-myc and LEF1, it becomes evident that the presence of germline and somatic mutations tilts the balance towards heightened expression of oncogenic proteins.

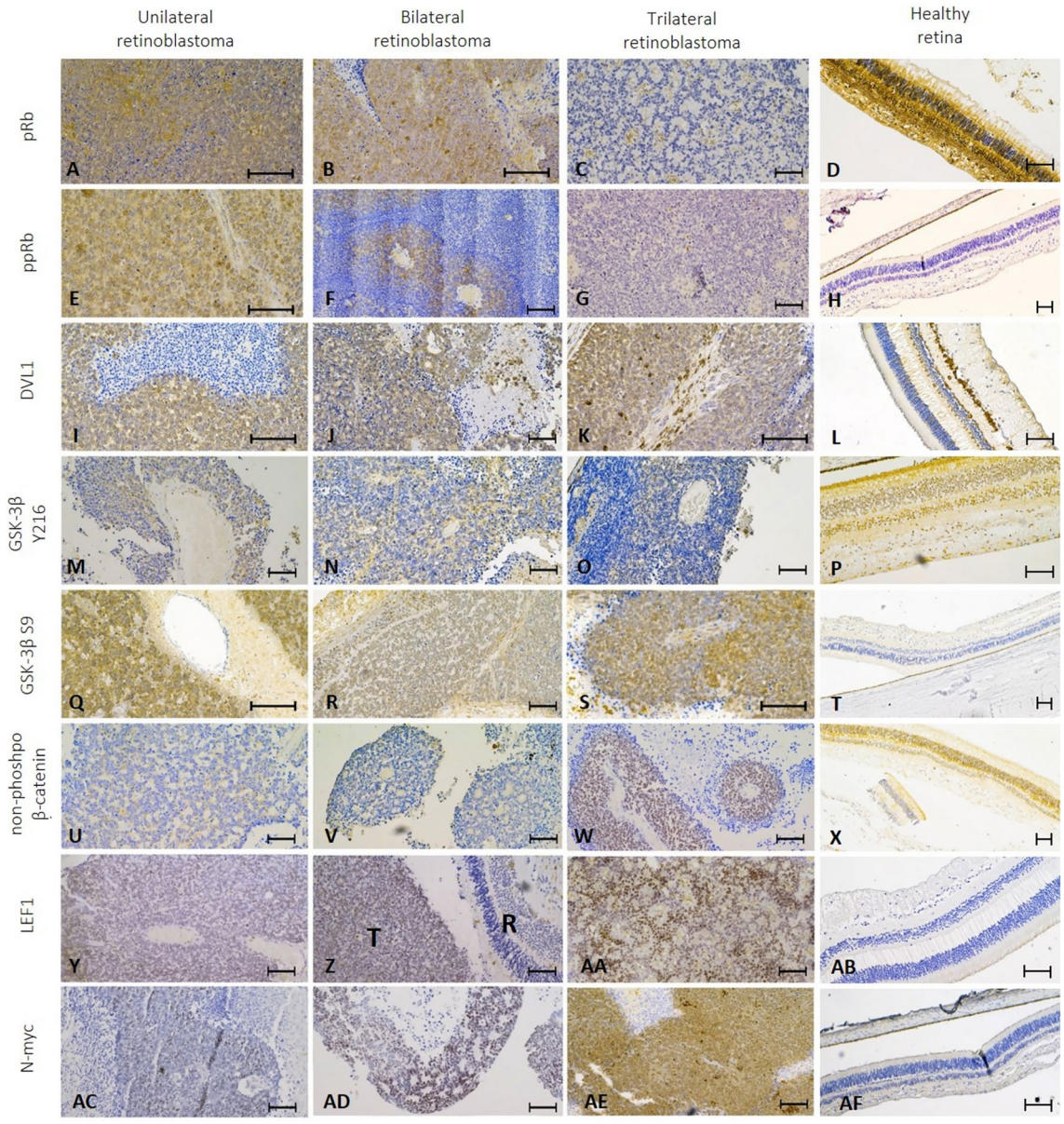

Fig. 3. Expression of pRb, ppRb, DVL1, GSK3β S9, GSK3β Y216, non-phospho β-catenin, LEF1 and N-myc in different types of retinoblastoma identified by immunostaining with antibodies against the analyzed proteins. Strong nuclear and cytoplasmic staining of pRb was observed in both unilateral and bilateral retinoblastoma tissues (**A**,**B**), as well as in healthy retina tissue (**D**). In contrast, trilateral retinoblastoma (**C**) displayed no pRb expression. Similarly, no ppRb expression was detected in healthy retina tissue (**H**), while unilateral and bilateral retinoblastomas (**E**,**F**) showed a range of ppRb expression from strong to weak. Strong DVL1 expression was evident in both the cytoplasm and nucleus of tumor cells (**I**–**K**), whereas no DVL1 expression was detected in healthy retina (**L**). In terms of GSK3β Y216, strong cytoplasmic expression was observed in healthy retina tissue (**P**), compared to the weaker expression noted in retinoblastoma tissues (**M**–**O**). Conversely, retinoblastoma tissues (**Q**–**S**) exhibited strong nuclear and cytoplasmic expression of GSK3β S9, while its expression was absent in healthy retina tissue (**T**). Non-phosphorylated β-catenin exhibited weak cytoplasmic expression in unilateral (**U**) and bilateral (**V**) retinoblastoma, whereas strong nuclear expression was noted in trilateral retinoblastoma (**W**). In healthy retina (**X**), strong cytoplasmic expression of non-P β-catenin was observed. LEF1 demonstrated moderate to strong nuclear expression in retinoblastoma tissues (**Y**,**Z**,**AA**), with no expression in healthy retina (**AB**). Trilateral retinoblastoma (**AE**) exhibited strong cytoplasmic and nuclear N-myc, while bilateral (**AD**) and unilateral (**AC**) retinoblastomas showed moderate to weak nuclear expression. N-myc was not expressed in healthy retina (**AF**). Scale bars correspond to 60 µm. Abbreviations: retina tissue (R), tumor tissue (T).

			IRS score (rounded average)		
	RB1 germline mutation status; sample percentage	pRb	ppRb	N-myc	LEF1
Unilateral retinoblastoma	$RB1^{+/+}$; (78%)	9	5	4	5
	$RB1^{+/-}$; (22%)	4	2	1	4
Bilateral retinoblastoma	$RB1^{+/+}$; (33%)	10	8	8	11
	$RB1^{+/-}$; (66%)	5	4	4	2
Trilateral retinoblastoma	$RB1^{+/+}$; (0%)	-	-	-	-
	$RB1^{+/-}$; (100%)	5	3	8	6

Table 3. Immunohistochemistry expression of pRb, ppRb, N-myc and LEF1 in unilateral, bilateral and trilateral retinoblastoma based on different *RB1* mutation status.

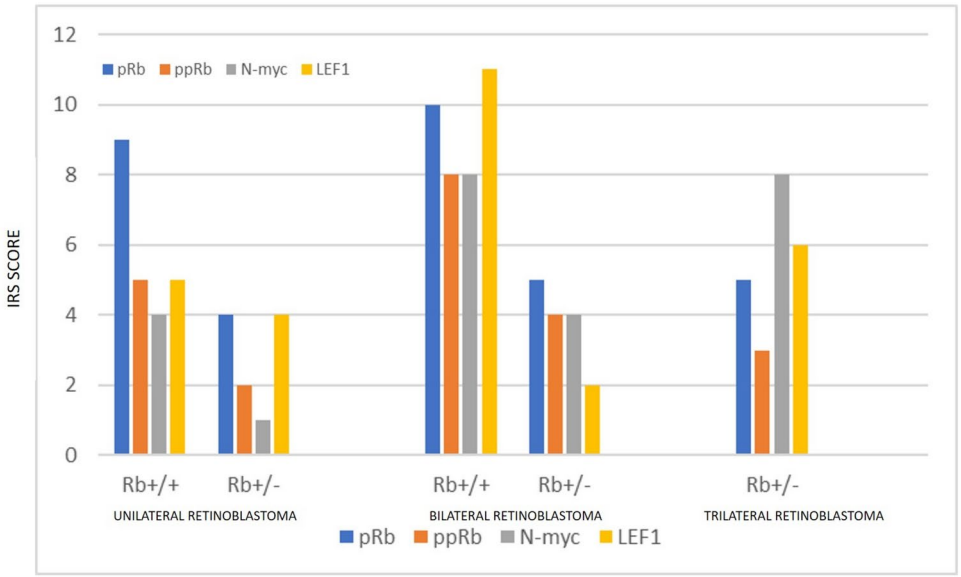

Fig. 4. Immunohistochemical analysis (expressed as a percentage of total) depicting the expression levels of the tumor suppressor protein pRb alongside the oncogenic proteins N-myc and LEF1 across unilateral, bilateral, and trilateral retinoblastoma cases stratified by distinct *RB1* mutation statuses.

Particularly noteworthy is the pronounced imbalance observed in trilateral retinoblastoma, where the expression levels of pRb, serving as a tumor suppressor protein, markedly differ from those of the oncogenic proteins N-myc and LEF1, as depicted in Fig. 4.

Also, it is important to note that all the mutations found in our sample were previously reported as we have verified with several databases: the LOVD (Leiden Open Variation Database) database, the Human Gene Mutation Database, ClinVar, InterVar, and Exome Aggregation Consortium, Mutation Taster (http://www.mutationtaster.org/) and Deleterious (Mutation taster, CADD) PROVEAN (http://provean.jcvi.org).

Discussion

Since evolving treatment approaches shift away from enucleation as the standard treatment, to an increasing focus on eye-preserving therapies, the opportunity to obtain enucleated tissue samples has become challenging. This change in treatment paradigm makes our collection especially valuable, as tissue availability has decreased due to more conservative therapeutic approaches designed to preserve the eye.

The collection of 22 tissue samples represents a significant portion of the diagnosed enucleated cases, which is particularly notable in light of the low incidence of this disease in Croatia with only 2 to 3 new cases per year. In spite of the limited number of cases, the consistency of our results on the present collection of retinoblastoma provides a solid foundation for advancing scientific understanding. The intricate process of embryonic development and the maturation of the central nervous system, particularly in structures like the retina, underscores the pivotal regulatory role of the canonical Wnt/β-catenin signaling pathway[22,23]. In this context, our study examines the expression changes of key proteins involved in the Wnt signaling pathway across different types of retinoblastoma and positions them in relation to pRB, ppRB and N-myc expression levels.

The rationale for studying retinoblastoma (RB) as unilateral, bilateral, and trilateral, rather than based solely on histopathological risk factors, lies in the distinct biological, clinical, and genetic characteristics associated with each form. The classification of retinoblastoma into unilateral, bilateral, and trilateral presentations

is imperative for comprehensively understanding its genetic implications, guiding treatment strategies, evaluating risks of secondary tumors, and improving prognosis through early detection[24–26]. Retinoblastoma, comprising approximately 3% of childhood cancers in individuals under 15 years old, is a relatively uncommon tumor[27]. Unilateral involvement, affecting one eye, predominates, while bilateral cases, impacting both eyes, are less frequent and often associated with germline mutations in the *RB1* gene[27]. Trilateral retinoblastoma, characterized by a third intracranial tumor, typically a PNET, in addition to bilateral retinoblastoma, is even rarer, occurring in only a minority of patients, estimated at approximately 1.5–5%[28]. In our study, the majority of cases demonstrated unilateral presentation (64%), while trilateral involvement was in 9% of cases. Furthermore, concerning the 8th edition of AJCC staging, unilateral retinoblastoma showcased the lowest grades in cTNM staging, predominantly manifesting as H0, indicating normal *RB1* alleles in blood tested with high sensitivity assays. Conversely, bilateral and trilateral cases were associated to higher grades, and both were associated with a positive heritable trait. Recent studies on correlation of prognostic tumor markers expression with TNM staging proved that high grade retinoblastoma showed moderate to strong immunoreactivity of oncogenic tumor markers (CD24)[29], which is in concordance with our results on staging grades in our cohort of unilateral, bilateral and trilateral retinoblastoma.

The initiation of retinoblastoma involves a cascade of genetic and epigenetic alterations that disrupt cellular homeostasis, leading to uncontrolled proliferation outside the normal niche. This dysregulation primarily occurs through the disruption of critical signaling pathways, including Rb, p53, Wnt, and Ras-ERK[30]. Knudson's pioneering work fundamentally transformed our understanding of retinoblastoma[31] and laid the foundation for identifying the activity of the *RB1* tumor-suppressor gene.

In most cases of non-hereditary retinoblastoma, unilateral tumors arise due to somatic pathogenic mutations in the *RB1* gene, resulting in the biallelic inactivation of this gene in retinal precursor cells[32]. Although recent advancements in high-throughput research have revealed a wide spectrum of pathogenic *RB1* variants[28,32,33], including particularly prevalent nonsense mutations that are associated with protein downregulation, our understanding of the mutational landscape of retinoblastoma remains incomplete.

Additionally, emerging evidence suggests that the Wnt signaling pathway may play a crucial role in regulating stem cell renewal and driving tumor formation in retinoblastoma, with recent studies further supporting its significance in retinoblastoma cell biology[34–38]. Our findings substantiate that the Wnt signaling pathway displays heightened activity in retinoblastoma cells in contrast to healthy retinal cells. Notably, levels of LEF1 expression are markedly elevated in cells of the unilateral ($BF_{10}=1.504$, error %=0.003), bilateral (BF = 1.433, error %=0.012, and trilateral ($BF_{10}=352.609$), error %= 2.664×10-^{4}) retinoblastoma compared to healthy retinal tissue. Moreover, distinctions in the active variant of β-catenin are evident between retinoblastoma and healthy retinal cells. β-catenin's role in healthy cells primarily involves functional cell-to-cell adhesion, while in tumor cells, it serves as a mediator of the Wnt pathway activation[39]. When β-catenin is not phosphorylated, it stabilizes in the cytoplasm and, consequently, passes into the nucleus serving as transcription regulator together with LEF1. In accordance is our finding on the correlation of expression levels in retinoblastoma cells between LEF1 and β-catenin (Pearson's $r=0.770$; $BF_{10}=982.387$) which confirmed their close relationship. Remarkably, in retinoblastoma, we observed a different localization pattern of β-catenin, with nuclear expression in retinoblastoma cells and cytoplasmic localization in retinal cells, as depicted in Fig. 1. Glycogen synthase kinase-3β (GSK3β) is pivotal in the Wnt signaling pathway. It regulates the pathway by activating Wnt signaling through phosphorylation of LRP 5/6 and β-catenin, and inhibiting GSK3β activity allows β-catenin to accumulate, translocate to the nucleus, and initiate the transcription of Wnt target genes[40]. Analyzing the expression levels of the active (GSK3β Y216) and inactive (GSK3β S9) forms provided valuable insights, notably indicating a prevalence of the inactive form within tumor cells. This observation corroborates existing evidence linking GSK3β's inactive state to the inability to destroy β-catenin thus establishing its role in tumorigenesis[41]. Furthermore, the notable disparity in expression levels between tumor cells and healthy retinal cells, underscored by a high Bayes factor ($BF_{10}=1568.09$; error $\% = 4.735\times10^{-7}$), suggests its potential utility as a novel marker and therapeutic target. Another pivotal protein in the Wnt signaling pathway cascade, DVL1, exhibited elevated expression levels in retinoblastoma cells compared to healthy retinal cells ($BF_{10}=14.69$; error $\% = 4.506\times10^{-5}$). Particularly in trilateral retinoblastoma, it demonstrated the most substantial deviation from healthy eyes retinal cell expression levels ($BF_{10}=52.239$; error $\% = 1.702\times10^{-5}$).

Demonstrating the up-regulation of the Wnt pathway in retinoblastoma, it is noteworthy to indicate that prominent target genes of β-catenin include *MYCC, MYCN, Cyclin D, LEF1, AXIN2, PPARdelta, VEGF, Survivin*, and others[42]. Recent investigations have identified a previously unrecognized form of retinoblastoma characterized by the absence of *RB1* mutations and the presence of functional protein activity, likely induced by the amplification of the *MYCN* oncogene[43]. This MYCN-driven retinoblastoma, constituting 2% of non-hereditary cases, typically presents as an early-onset, unilateral tumor diagnosed around 4.5 months of age[44]. Moreover, Hun et al. examined *MYCN* gene amplification in retinoblastoma through in situ hybridization on 26 unilateral sporadic human retinoblastoma samples. Their results suggest that *MYCN* proto-oncogene amplification may be a defining characteristic of certain subtypes of retinoblastoma[45]. This role of MYCN was further corroborated by Saengwimol et al., who identified *MYCN* amplification as the primary driver in this novel subtype of retinoblastoma, which is devoid of *RB1* gene mutations and non-phosphorylated RB1 protein. This subtype exhibits a more aggressive clinical course compared to traditional RB1-deficient retinoblastoma[13]. Notably, our findings revealed strong positive immunostaining for N-myc in over one-third of the analyzed cases.

Reflecting on these findings, Osorio[46] proposes that in the absence of functional pRb, factors such as MYCN and E2Fs undergo a process of "repurposing," contributing to uncontrolled cell proliferation. Our findings align with this perspective, illustrating how in retinoblastoma with germline mutations, particularly bilateral and trilateral cases, the equilibrium between tumor suppressor protein expression (pRb) and oncogene activity

(LEF1 and N-myc) tilts toward oncogenes, culminating in more aggressive tumors, as evidenced by their higher cTNM grade. Our descriptive study did not investigate mechanisms behind the observed changes and we leave this work for future studies. While *RB1* inactivation through mutations has traditionally been linked with retinoblastoma, dysregulation of additional pathways common across various human cancers may also contribute to tumor etiology[9,47].

Conclusion

In summary, our results highlight the up-regulation of the Wnt/β-catenin pathway and N-myc, uncovering novel molecular changes underlying retinoblastoma etiology. The study offers valuable insights for future research endeavors aimed at enhancing our comprehension of retinoblastoma pathogenesis and identifying reliable biomarkers and molecular targets to advance diagnostic and therapeutic strategies. Molecular findings when integrated with clinical and pathological data, can improve our understanding of retinoblastoma behavior.

Data availability

All data generated or analysed during this study are included in this published article.

Received: 30 June 2024; Accepted: 2 December 2024
Published online: 30 December 2024

References

1. Aerts, I. et al. Retinoblastoma. *Orphanet J. Rare Dis.* **1**, 31. https://doi.org/10.1186/1750-1172-1-31 (2006).
2. Kamihara, J. et al. Retinoblastoma and neuroblastoma predisposition and surveillance. *Clin. Cancer Res.* **23**, e98–e106. https://doi.org/10.1158/1078-0432.CCR-17-0652 (2017).
3. Cancer Research UK. About retinoblastoma. Cancer Research UK. [Accessed 17 June 2024]. Available at: https://www.cancerresearchuk.org/about-cancer/childrens-cancer/eye-cancer-retinoblastoma/about
4. TNM8: The updated TNM classification for retinoblastoma. *Community Eye Health* **31**, 34 (2018).
5. Yun, J., Li, Y., Xu, C. T. & Pan, B. R. Epidemiology and Rb1 gene of retinoblastoma. *Int. J. Ophthalmol.* **4**, 103–109. https://doi.org/10.3980/j.issn.2222-3959.2011.01.24 (2011).
6. Indovina, P. et al. RB1 dual role in proliferation and apoptosis: Cell fate control and implications for cancer therapy. *Oncotarget* **6**, 17873–17890. https://doi.org/10.18632/oncotarget.4286 (2015).
7. Lee, C. & Kim, J. K. Chromatin regulators in retinoblastoma: Biological roles and therapeutic applications. *J. Cell Physiol.* **236**, 2318–2332. https://doi.org/10.1002/jcp.30022 (2021).
8. Tell, S., Yi, H., Jockovich, M. E., Murray, T. G. & Hackam, A. S. The Wnt signaling pathway has tumor suppressor properties in retinoblastoma. *Biochem. Biophys. Res. Commun.* **349**, 261–269. https://doi.org/10.1016/j.bbrc.2006.08.044 (2006).
9. Harbour, J. W. & Dean, D. C. The Rb/E2F pathway: Expanding roles and emerging paradigms. *Genes Dev.* **14**, 2393–2409. https://doi.org/10.1101/gad.813200 (2000).
10. Xiao, W., Chen, X. & He, M. Inhibition of the Jagged/Notch pathway inhibits retinoblastoma cell proliferation via suppressing the PI3K/Akt, Src, p38MAPK and Wnt/β-catenin signaling pathways. *Mol. Med. Rep.* https://doi.org/10.3892/mmr.2014.2213 (2014).
11. Li, Z., Li, Q. & Wang, G., et al. Inhibition of Wnt/β-catenin by anthelmintic drug niclosamide effectively targets growth, survival, and angiogenesis of retinoblastoma. *Am. J. Transl. Res.* 3776–3786. (2017).
12. He, H. & Qin, M. Long non-coding RNA LEF1-AS1 is involved in the progression of retinoblastoma through regulating the Wnt/β-catenin pathway. *Clin. Exp. Pharmacol. Physiol.* https://doi.org/10.1111/1440-1681.13263 (2020).
13. Saengwimol, D. et al. Silencing of the long noncoding RNA MYCNOS1 suppresses activity of MYCN-amplified retinoblastoma without RB1 mutation. *Investig. Ophthalmol. Vis. Sci.* https://doi.org/10.1167/iovs.61.14.8 (2020).
14. Kafka, A. et al. Methylation patterns of DKK1, DKK3 and GSK3β are accompanied with different expression levels in human astrocytoma. *Cancers (Basel).* https://doi.org/10.3390/cancers13112530 (2021).
15. Kafka, A. et al. Different behaviour of DVL1, DVL2, DVL3 in astrocytoma malignancy grades and their association to TCF1 and LEF1 upregulation. *J. Cell. Mol. Med.* https://doi.org/10.1111/jcmm.13969 (2019).
16. Pećina-Šlaus, N. et al. Wnt signaling transcription factors TCF-1 and LEF-1 are upregulated in malignant astrocytic brain tumors. *Histol. Histopathol.* https://doi.org/10.14670/HH-29.1557 (2014).
17. Bao, J., Lee, H. J. & Zheng, J. J. Genome-wide network analysis of Wnt signaling in three pediatric cancers. *Sci Rep.* https://doi.org/10.1038/srep02969 (2013).
18. Choudhary, S., Singh, M. K., Kashyap, S., Seth, R. & Singh, L. Wnt/β-catenin signaling pathway in pediatric tumors: Implications for diagnosis and treatment. *Children (Basel).* https://doi.org/10.3390/children11060700 (2024).
19. Gao, Y., Chen, X. & Zhang, J. LncRNA MEG3 inhibits retinoblastoma invasion and metastasis by inducing β-catenin degradation. *Am. J. Cancer Res.* (2022).
20. Chen, X., Ouyang, L., Ke, N., Pi, L. & Zhou, X. Study on the role of MYCN in retinoblastoma by inhibiting p53 and activating wnt/βcatenin/Fra-1 signaling pathway by reducing DKK3. *Drug Dev. Res.* https://doi.org/10.1002/ddr.22222 (2024).
21. Ewens, K. G. et al. Phosphorylation of pRb: Mechanism for RB pathway inactivation in MYCN-amplified retinoblastoma. *Cancer Med.* **6**, 619–630. https://doi.org/10.1002/cam4.1010 (2017).
22. Kassumeh, S. et al. The neuroprotective role of Wnt signaling in the retina. *Neural Regen. Res.* **16**, 1524–1528. https://doi.org/10.4103/1673-5374.303010 (2021).
23. Pecina-Slaus, N. et al. Wnt signaling transcription factors TCF-1 and LEF-1 are upregulated in malignant astrocytic brain tumors. *Histol. Histopathol.* **29**, 1557–1564. https://doi.org/10.14670/HH-29.1557 (2014).
24. de Jong, M. C. et al. Trilateral retinoblastoma: A systematic review and meta-analysis. *Lancet Oncol.* **15**, 1157–1167. https://doi.org/10.1016/S1470-2045(14)70336-5 (2014).
25. Ancona-Lezama, D., Dalvin, L. A. & Shields, C. L. Modern treatment of retinoblastoma: A 2020 review. *Indian J. Ophthalmol.* **68**, 2356–2365. https://doi.org/10.4103/ijo.IJO_721_20 (2020).
26. Rodjan, F. et al. Trilateral retinoblastoma: neuroimaging characteristics and value of routine brain screening on admission. *J. Neurooncol.* **109**, 535–544. https://doi.org/10.1007/s11060-012-0922-4 (2012).
27. PDQ Pediatric Treatment Editorial Board. Retinoblastoma Treatment (PDQ): Health Professional Version. In: PDQ Cancer Information Summaries. Bethesda (MD): National Cancer Institute (US); January 4, 2024.
28. Frenkel, S. et al. Genotype-phenotype correlation in the presentation of retinoblastoma among 149 patients. *Exp. Eye Res.* **146**, 313–317. https://doi.org/10.1016/j.exer.2016.04.002 (2016).
29. Ishaq, S. M. et al. Correlation of CD24 expression with histological grading and TNM staging of retinoblastoma. *Pak. J. Med. Sci.* **32**, 160–164. https://doi.org/10.12669/pjms.321.8828 (2016).

30. Byroju, V. V. et al. Retinoblastoma: Present scenario and future challenges. *Cell Commun. Signal.* **21**, 226. https://doi.org/10.1186/s12964-023-01223-z (2023).
31. Knudson, A. G. Mutation and cancer: Statistical study of retinoblastoma. *Proc. Natl Acad. Sci. USA* **68**, 820–823. https://doi.org/10.1073/pnas.68.4.820 (1971).
32. Soliman, S. E. et al. Genetics and molecular diagnostics in retinoblastoma-an update. *Asia Pac. J. Ophthalmol. (Phila)* **6**, 197–207. https://doi.org/10.22608/APO.201711 (2017).
33. Tomar, S. et al. Mutation spectrum of RB1 mutations in retinoblastoma cases from Singapore with implications for genetic management and counselling. *PLoS ONE* **12**, e0178776. https://doi.org/10.1371/journal.pone.0178776 (2017).
34. Wu, T. et al. SOST silencing promotes proliferation and invasion and reduces apoptosis of retinoblastoma cells by activating Wnt/beta-catenin signaling pathway. *Gene Ther.* **24**, 399–407. https://doi.org/10.1038/gt.2017.31 (2017).
35. Lohmann, D. R. & Gallie, B. L. Retinoblastoma. 2000 Jul 18 [updated 2023 Sep 21]. In: Adam, M. P. et al. (eds) GeneReviews¬Æ. Seattle (WA): University of Washington, Seattle; 1993–2024.
36. Xu, L. et al. LncRNA MBLN1-AS1 inhibits the progression of retinoblastoma through targeting miR-338-5p-Wnt/β-catenin signaling pathway. *Inflamm. Res.* **70**, 217–227. https://doi.org/10.1007/s00011-020-01432-z (2021).
37. Liu, B., Gao, T., Wu, H. Y. & Wan, M. Erb-B2 receptor tyrosine kinase 2 knockdown inhibits retinoblastoma progression via Wnt/beta-catenin signaling pathway in vitro. *J. Biol. Regul. Homeost. Agents* **35**, 209–214. https://doi.org/10.23812/20-594-L (2021).
38. Bai, S., Shao, J., Bi, C. & Li, F. beta-asarone attenuates the proliferation, migration and enhances apoptosis of retinoblastoma through Wnt/beta-catenin signaling pathway. *Int. Ophthalmol.* **43**, 1687–1699. https://doi.org/10.1007/s10792-022-02566-1 (2023).
39. Liu, J. et al. Wnt/beta-catenin signalling: Function, biological mechanisms, and therapeutic opportunities. *Signal Transduct. Target Ther.* **7**, 3. https://doi.org/10.1038/s41392-021-00762-6 (2022).
40. Khurana, C. & Bedi, O. Proposed hypothesis of GSK-3Œ≤ inhibition for stimulating Wnt/β-catenin signaling pathway which triggers liver regeneration process. *Naunyn Schmiedebergs Arch. Pharmacol.* **395**, 377–380. https://doi.org/10.1007/s00210-022-02207-5 (2022).
41. Kaidanovich-Beilin, O. & Woodgett, J. R. GSK-3: Functional insights from cell biology and animal models. *Front. Mol. Neurosci.* **4**, 40. https://doi.org/10.3389/fnmol.2011.00040 (2011).
42. Herbst, A. et al. Comprehensive analysis of β-catenin target genes in colorectal carcinoma cell lines with deregulated Wnt/β-catenin signaling. *BMC Genomics* **15**, 74. https://doi.org/10.1186/1471-2164-15-74 (2014).
43. Rushlow, D. E. et al. Characterisation of retinoblastomas without RB1 mutations: Genomic, gene expression, and clinical studies. *Lancet Oncol.* **14**, 327–334. https://doi.org/10.1016/S1470-2045(13)70045-7 (2013).
44. Markovic, L. et al. Genetics in ophthalmology: Molecular blueprints of retinoblastoma. *Hum. Genomics* **17**, 82. https://doi.org/10.1186/s40246-023-00529-w (2023).
45. Kim, J. H. et al. N-myc amplification was rarely detected by fluorescence in situ hybridization in retinoblastoma. *Hum. Pathol.* **39**(8), 1172–1175. https://doi.org/10.1016/j.humpath.2007.12.008 (2008).
46. Osorio, J. Cell cycle: Repurposing MYC and E2F in the absence of RB. *Nat. Rev. Mol. Cell Biol.* **16**, 516–517. https://doi.org/10.1038/nrm4044 (2015).
47. Lee, W. H., Murphree, A. L. & Benedict, W. F. Expression and amplification of the N-myc gene in primary retinoblastoma. *Nature* **309**, 458–460. https://doi.org/10.1038/309458a0 (1984).

Author contributions

NPŠ and LM conceptualized and wrote the manuscript, AB, BP, FD, LM carried out the molecular studies. AMV, AB and LM drafted the manuscript and critically revised the manuscript. DT, AJ, BP and RH analyzed and interpreted the immunostaining results and contributed to editing. ZS statistically analyzed the data. LM and AMV provided the figures. NPŠ and RH supervised and secured funding. All authors read and approved the final manuscript.

Funding

The Scientific Centre of Excellence for Basic, Clinical and Translational Neuroscience (project GA KK01.1.1.01.0007 funded by the European Union through the European Regional Development Fund); University of Zagreb scientific funds no. 10106-23-2393 and 10106-24-1546; Croatian Science Foundation, IP2016-06-8636.

Declarations

Competing interests

The authors declare no competing interests.

Ethics approval and consent to participate

The Ethics Committees of the School of Medicine, University of Zagreb (Case number: 380-59-10106-20-111/126; Class: 641-01/20-02/01), University Hospital Center Zagreb (Case number: 02/21 AG; Class: 8.1-20/108-2), University Hospital Center „Sestre Milosrdnice " (Case number: 251-29-11-20-01-9; Class: 003-06/20-03/015), and Univerity Hospital „Sveti Duh" (Case number: 012-5477) have approved the research. The study adhered to the principles outlined in the Declaration of Helsinki with patients consent to participate. I confirm that informed consent was obtained from all subjects.

Additional information

Supplementary Information The online version contains supplementary material available at https://doi.org/10.1038/s41598-024-82044-z.

Correspondence and requests for materials should be addressed to N.P.-Š.